INTRODUCTION

This note describes the basis for a dynamic computer simulation of an axisymmetric free-surface liquid metal MHD flow with galvanically driven electrical currents. The goal is to eventually use a later version of this computer simulation within the APEX&ALPS study efforts as a tool to investigate and evaluate various proposed free-surface flowing LMMHD blanket design concepts for possible application in tokamak magnetic fusion reactors. In these proposed design concepts, liquid metal (preferably lithium) enters the toroidal chamber enclosing a tokamak plasma, through two toroidally continuous slits located at the chamber's top. As the liquid metal flows to the chamber's bottom it is held against the chamber's walls and away from the plasma by a magnetic restraining force developed within the bulk liquid metal, which acts in conjunction with gravitational and centrifugal force effects. After reaching the chamber's bottom, the liquid metal exits through one or more toroidally continuous slits provided for that purpose.

The magnetic restraining force density, a "body force", is developed within the bulk liquid metal through J X B interactions between the externally generated toroidal field, which must be present for any tokamak, and poloidal electric currents which are galvanically driven in the liquid metal for this restraining force purpose.

Figure 1: General Electromagnetic Restraint Scheme

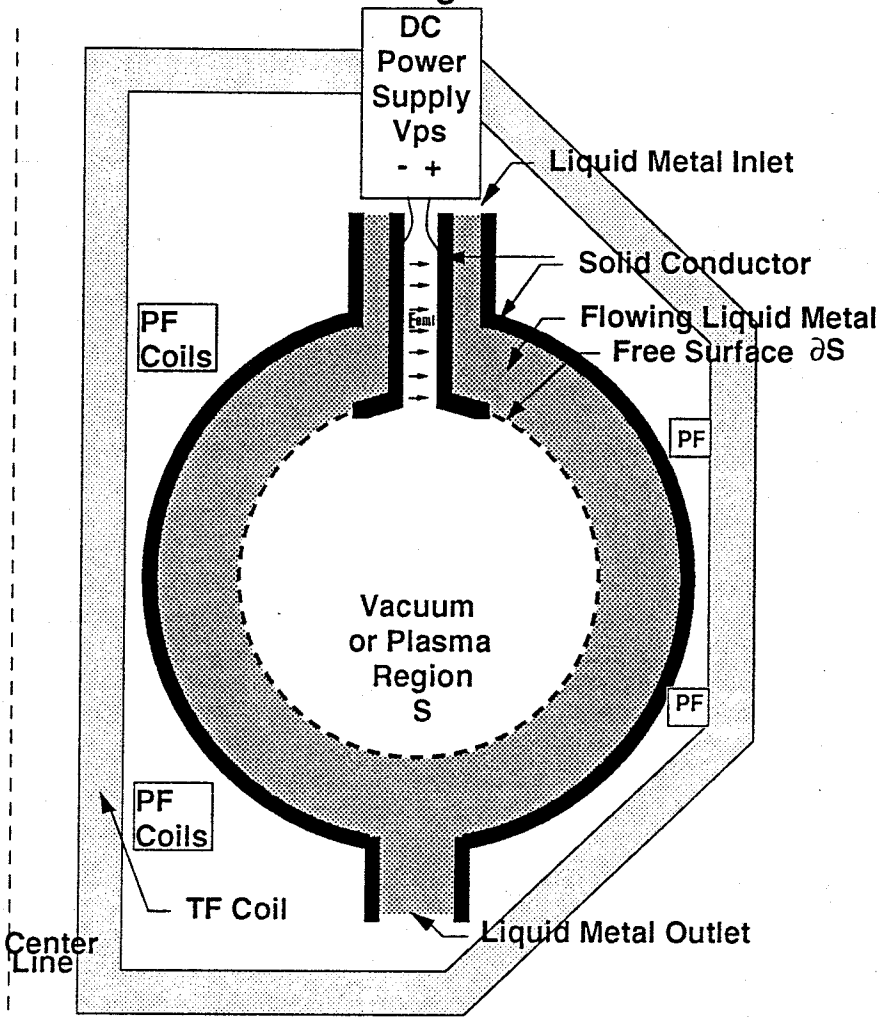

$$\frac{\partial u_z}{\partial t} = -u_r \frac{\partial u_z}{\partial r} - u_z \frac{\partial u_z}{\partial z} - \frac{1}{\rho}\frac{\partial p}{\partial z} + \nu\left(\frac{1}{r}\frac{\partial}{\partial r}\left(r\frac{\partial u_z}{\partial r}\right) + \frac{\partial^2 u_z}{\partial z^2}\right) + g_z - \frac{J_\varphi B_r}{\rho} - \frac{\mu I}{4\pi^2 r^2 \rho}\frac{\partial I}{\partial z} \tag{41}$$

However, the toroidal component of current is related to the poloidal flux via

$$\mu J_\varphi \hat{\varphi} = \nabla \times \vec{B}_P$$
$$= \nabla \times \left(\nabla \times \left(\frac{\Psi \hat{\varphi}}{2\pi r}\right)\right)$$
$$= -\vec{\nabla}^2\left(\frac{\Psi \hat{\varphi}}{2\pi r}\right)$$

so that

$$J_\varphi = -\frac{1}{2\pi r \mu}\Delta^* \Psi \tag{42}$$

where $\Delta^* := r\frac{\partial}{\partial r}\frac{1}{r}\frac{\partial}{\partial r} + \frac{\partial^2}{\partial z^2}$ is the Grad-Shafranov operator, again. Substituting Equations (42) and (21), the velocity evolution equations become:

$$\frac{\partial u_r}{\partial t} = \frac{u_\varphi^2}{r} - u_r \frac{\partial u_r}{\partial r} - u_z \frac{\partial u_r}{\partial z} - \frac{1}{\rho}\frac{\partial p}{\partial r} + \nu\left(\frac{1}{r}\frac{\partial}{\partial r}\left(r\frac{\partial u_r}{\partial r}\right) + \frac{\partial^2 u_r}{\partial z^2} - \frac{u_r}{r^2}\right) - \frac{\Delta^* \Psi}{4\pi^2 r^2 \rho \mu}\frac{\partial \Psi}{\partial r} - \frac{\mu I}{4\pi^2 r^2 \rho}\frac{\partial I}{\partial r} \tag{43}$$

$$\frac{\partial u_\varphi}{\partial t} = -\frac{u_r u_\varphi}{r} - u_r \frac{\partial u_\varphi}{\partial r} - u_z \frac{\partial u_\varphi}{\partial z} + \nu\left(\frac{1}{r}\frac{\partial}{\partial r}\left(r\frac{\partial u_\varphi}{\partial r}\right) + \frac{\partial^2 u_\varphi}{\partial z^2} - \frac{u_\varphi}{r^2}\right) + \frac{1}{4\pi^2 r^2 \rho}\left(\frac{\partial I}{\partial z}\frac{\partial \Psi}{\partial r} - \frac{\partial I}{\partial r}\frac{\partial \Psi}{\partial z}\right\} \tag{44}$$

$$\frac{\partial u_z}{\partial t} = -u_r \frac{\partial u_z}{\partial r} - u_z \frac{\partial u_z}{\partial z} - \frac{1}{\rho}\frac{\partial p}{\partial z} + \nu\left(\frac{1}{r}\frac{\partial}{\partial r}\left(r\frac{\partial u_z}{\partial r}\right) + \frac{\partial^2 u_z}{\partial z^2}\right) + g_z - \frac{\Delta^* \Psi}{4\pi^2 r^2 \rho \mu}\frac{\partial \Psi}{\partial z} - \frac{\mu I}{4\pi^2 r^2 \rho}\frac{\partial I}{\partial z} \tag{45}$$

In order to enforce the divergence-free velocity condition, the pressure field must in general have a particular non-zero divergence . Taking the divergence of Equation (34) and requiring that $\nabla \bullet \bar{u} = 0 \Rightarrow \nabla \bullet \frac{\partial \bar{u}}{\partial t} = 0$, we get the Pressure Poisson Equation:

$$\nabla^2 p = -\rho \nabla \bullet [(\bar{u} \bullet \nabla)\bar{u}] + \nabla \bullet (\bar{J} \times \bar{B}) \tag{46}$$

where spatially constant density and kinematic viscosity have been assumed. In component form this can be rewritten as:

$$\boxed{\begin{aligned}\nabla^2 p = -\rho\Big(&\frac{1}{r}\frac{\partial}{\partial r}\Big(r\Big[\frac{u_\varphi^2}{r} - u_r\frac{\partial u_r}{\partial r} - u_z\frac{\partial u_r}{\partial z}\Big]\Big) + \frac{\partial}{\partial z}\Big[-u_r\frac{\partial u_z}{\partial r} - u_z\frac{\partial u_z}{\partial z}\Big]\Big) \\ &- \frac{1}{4\pi^2 r\rho}\Big(\frac{\partial}{\partial r}\Big(\frac{1}{r}\Big[\frac{\Delta^* \Psi}{\mu}\frac{\partial \Psi}{\partial r} + \mu I\frac{\partial I}{\partial r}\Big]\Big) + \frac{\partial}{\partial z}\Big(\frac{1}{r}\Big[\frac{\Delta^* \Psi}{\mu}\frac{\partial \Psi}{\partial z} + \mu I\frac{\partial I}{\partial z}\Big]\Big)\Big)\end{aligned}} \tag{47}$$

The evolution equation for poloidal flux is obtained by substituting Equations (21) and (42) into (24) and combining terms:

$$\boxed{\frac{\partial \Psi}{\partial t} = -u_r\frac{\partial \Psi}{\partial r} - u_z\frac{\partial \Psi}{\partial z} + \frac{1}{\sigma\mu}\Delta^* \Psi} \tag{48}$$

Boundary conditions for poloidal flux are implemented via the MacDonald-Wexler algorithm, which uses Greens functions related to the finite region boundary.

The free-surface grid boundary must itself move to follow the perpendicular motion of the fluid. The required velocity of the grid boundary, $\bar{v}_b$, is

$$\boxed{\bar{v}_b = (\bar{u} \bullet \hat{n})\hat{n}} \tag{49}$$

where $\hat{n}$ is the unit vector perpendicular to the free surface.

Figure 1 is an axisymmetric elevation view (i.e., a poloidal, or meridional, half-plane) showing general aspects of the proposed design schemes for an electromagnetically restrained free-surface liquid metal blanket. The depicted features are to be represented in the computer simulation, although the initial (alpha0) version of the computer simulation omits some of the features. All simulation variables are modeled as having axisymmetric geometry, as is appropriate for LMMHD designs intended to operate in close proximity to the necessarily axisymmetric tokamak plasma's magnetic confinement geometry.

The fundamental simulation variables have been chosen in a novel manner which avoids any need to numerically integrate electromagnetic partial differential equations through vacuum regions, instead relying on analytical expressions to give boundary conditions on conducting material surfaces. The simulated electrical variables which do vary within conducting regions are the poloidal threading current and the poloidal magnetic flux. Although it would also in principle be possible to use a velocity stream function/ vorticity formulation for the axisymmetric flowing liquid metal, this simulation instead directly uses velocity components expressed in a (r,φ,z) cylindrical coordinate system, in order to reduce free surface boundary condition complications.

An adaptive unstructured grid is used in the simulation both to track the free surface boundary and also to resolve internal boundary layers without requiring an excessive number of grid points. The free surface boundary nodes are moved within each time step, following the free surface motion. Internal nodes are then reallocated, repositioned , and interpolated between time steps.

An unfortunate side effect of the adaptive grid's ability to resolve small features is that the resulting differential equations in time, although analytically stable , can become "stiff", i.e. they can develop some extremely fast dissipative time constants . Explicit numerical integration then becomes unstable unless the integration time steps are similarly small. To avoid this pathological behavior, the time integration method used throughout this simulation is the backwards (implicit) Euler method. This method has the advantages that it is unconditionally "A-stable" and is even "L-stable" as defined by Lambert, but has the disadvantage that its computational algorithm is considerably more complicated than explicit integration methods. For one instance, the incompressible flow dynamical equations couple the implicit solution of a future "Pressure Poisson Equation" with the implicit calculation of a future velocity field. For another, the motion and future position of the free surface boundary must be consistent with its future velocity. These implicit method algorithms are derived based on linearizations of the defining equations, and these linearized equations are efficiently solved via multigrid techniques. "Outer" Picard iteration substitutions in the nonlinear equations are employed to further improve accuracy.

In order to avoid intolerable complexity in the algorithm for moving free surface boundary nodes, the finite elements adjacent to the free surface should have a simple structure. In particular, complicated finite elements with internal nodes not on the free surface boundary and with associated higher order interpolation functions would require more sophisticated algorithms to implement free surface boundary motion than needed for piecewise linear interpolation on triangular cross section finite elements. To simplify the simulation, simple axisymmetric ring elements with triangular cross section and piecewise-linear C^0 continuity interpolation are used for all field variables throughout the computational domain.

Published literature documents various unsuccessful experiences in computing solutions to Navier-Stokes equations for incompressible fluid flow using Galerkin finite element formulations, with some reported problems being quite subtle. The most common Galerkin formulations include an integration by parts invoking Greens theorem, after which

the pressure term enters the formulas directly but only the first spatial derivatives of the velocity terms are included. "Spurious pressure modes" in the solution can result if the same degree of interpolating polynomials is used for both pressure and velocity; it is reported that they can be avoided by using a velocity interpolation polynomial of one higher degree than the polynomial used for pressure interpolation. It is also reported that "spurious pressure modes" are avoided by using an explicit "pressure projection" method, or by using the "least squares" finite element formulation instead of the Galerkin one. Another observed problem is "locking" which prevents finding a nonzero solution when an insufficiently rich set of interpolation functions for velocity are overconstrained by incompressible continuity requirements. "Locking" can also be grid-dependent, with the solutions found on coarse grids not converging as the grid is refined. Quadratic or cubic polynomial interpolation functions for velocity components have been successfully employed in computer codes avoiding both of these pathologies.

This simulation attempts to avoid such numerical difficulties while still using C^0 continuous piecewise linear interpolation for all fields, by using an unconventional Galerkin formulation for velocity and pressure in which Greens theorem is not invoked. Instead of integrating by parts to replace second derivatives by first derivatives, additional simulation variables are employed to separately estimate the first derivatives of the field variables with their own piecewise linear interpolation. Thus, in this formulation, spatial derivatives of the estimated field variables are different from estimates of the field variables' spatial derivatives. This general formulation was termed "Mixed Finite Element Approximation" by Lapidus and Pinder, but no references have been found documenting its performance track record with Navier-Stokes systems.

The following description is organized in four sections:

1) Definition of the fundamental simulation variables and derivation of their defining (partial) differential equations and boundary conditions.
2) Definition of the numerical algorithms.
3) Definition of the simulation program structure and modules.
4) Initial results from simulation.

SIMULATION VARIABLES AND EQUATION DERIVATIONS

We start with quasi-static electromagnetic field equations:

Ampere's Law:

$$\nabla \times \vec{B} = \mu \vec{J} \quad (\Rightarrow \nabla \bullet \vec{J} = 0) \tag{1}$$

Faraday's Law:

$$\nabla \times \vec{E} = -\frac{\partial \vec{B}}{\partial t} \tag{2}$$

Magnetic Vector Potential:

$$\nabla \bullet \vec{B} = 0 \quad \Leftrightarrow \quad \nabla \times \vec{A} = \vec{B} \tag{3}$$

Coulomb gauge for magnetic vector potential:

$$\nabla \bullet \vec{A} = 0 \tag{4}$$

Substituting vector potential into Faraday's Law yields

$$\nabla\times(\vec{E}+\frac{\partial\vec{A}}{\partial t})=0 \quad \Rightarrow \quad \vec{E}=-\frac{\partial\vec{A}}{\partial t}-\nabla V \tag{5a,5b}$$

where V is the voltage potential.

Ohm's Law:

$$\vec{J}=\sigma(\vec{E}+\vec{E}_{emf}+\vec{u}\times\vec{B}) \tag{6}$$

In Ohm's Law, the electromotive force (emf) of the electrical power supply has the mathematical form of a nonconservative electric field which is nonzero only in the space between the power supply terminals. It is not actually an electric field in the sense that the electromotive force does not directly contribute to Faraday's law. The vector field, $\vec{u}$, represents conductor velocity, and is generally nonzero for flowing liquid metal.

Combining the curl of Ohm's law with Faraday's law gives:

$$\frac{\partial\vec{B}}{\partial t}=\nabla\times(\vec{u}\times\vec{B})-\nabla\times\frac{\vec{J}}{\sigma}+\nabla\times\vec{E}_{emf} \tag{7}$$

It may seem paradoxical that in the case of two nested solenoid coil windings, either toroidal or infinitely long, a time varying current in the inner winding induces a voltage in the outer winding even though it produces identically zero magnetic field there. One explanation is found in Equation (5b) and in the fact that the vector potential, $\vec{A}$, does not vanish outside an infinite or toroidal solenoid despite the fact that $\vec{B}=\nabla\times\vec{A}$ does. Computer calculation using $\vec{A}$ as a field variable instead of $\vec{B}$ is conventional practice for time-varying magnetic situations such as those involving eddy curents. Another explanation is that the joint use of spatially continuous $\vec{B}$ and $\vec{E}$ fields for time varying situations does not fail on simply connected computational domains (i.e., domains which do not enclose any "computational holes" such as an inner nested solenoid excluded from computation).

The axisymmetric time-varying vector field variables to be computed are the fluid velocity , $\vec{u}$, and the magnetic induction, $\vec{B}$, represented in cylindrical component form as

$$\vec{u}=u_r\hat{a}_r+u_\varphi\hat{\varphi}+u_z\hat{a}_z$$
$$\vec{B}=B_r\hat{a}_r+B_\varphi\hat{\varphi}+B_z\hat{a}_z \tag{8a,8b}$$

Because of the impressive computational demands in calculating time-varying LMMHD flows, we do not want the computer to waste avoidable time and effort calculating electromagnetic fields in vacuum regions. We therefore seek a formulation in which the computational grid covers only the electrically conducting region, including liquid metal and solid metal subregions. This formulation requires replacing the magnetic field components with different but related scalar variables in the simulation, as developed below. The toroidal magnetic field component is redefined in terms of a "poloidal threading current" variable which has the distinction that it is spatially constant throughout vacuum regions. The toroidal field in the enclosed "computational hole" surrounded by liquid metal is replaced by a time-varying "trapped flux" variable which has no spatial variation. The poloidal magnetic field components are redefined in terms of the poloidal magnetic flux

variable, and a Greens function method is used to directly represent poloidal flux on the conducting computational region's boundary without calculating it in vacuum regions.

Because of axisymmetry, the toroidal field in a vacuum region varies exactly as

$$B_\varphi = \frac{B_0 R_0}{r} \tag{9}$$

for some value of B_0R_0. In a tokamak plasma the externally imposed toroidal field is typically much stronger than the variations in toroidal field caused by poloidal plasma currents, so the toroidal field still varies approximately as given by Equation (9) even when a tokamak plasma is present. As depicted in Figure 1, the contour ∂S lies in a poloidal plane and surrounds only the vacuum (i.e., plasma) region which is enclosed inside the metallic conducting region. Using Equation (9) to calculate the enclosed toroidal field magnetic flux gives:

$$\Phi = \int_S \frac{B_0 R_0}{r} dr\, dz = B_0 R_0 \oint_{\partial S} \frac{z}{r} dr \tag{10}$$

shouldn't this be $\int r\, d\varphi\, dr$?

where the integral around the Figure 1 contour, ∂S, is evaluated in the clockwise direction as per Stokes' theorem. This enclosed toroidal magnetic flux variable, Φ, cannot change instantaneously because it is surrounded by conducting material. It thus is an appropriate choice to use directly as a dynamic simulation state variable. Integrating the toroidal component of Equation (7) over the Figure 1 vacuum region, S, and invoking Stoke's theorem gives its time rate of change vs. the power supply voltage and other variables:

$$\frac{d\Phi}{dt} = V_{PS} - \oint_{\partial S} \frac{\vec{J}}{\sigma} \bullet d\vec{\ell} + \oint_{\partial S} \vec{u} \times \vec{B} \bullet d\vec{\ell} \tag{11}$$

In axisymmetric geometry, the total net poloidal "threading current" between the center line axis of symmetry and any (r,z) location, expressed in ampere-turns, is related to the local toroidal field, $B_\varphi(r,z)$, by

$$I(r,z) = \frac{2\pi}{\mu} r B_\varphi(r,z) \tag{12}$$

In particular, a single constant value of this threading current, I_s is valid for all locations throughout the enclosed vacuum region and its boundary:

$$I_s = \frac{2\pi}{\mu} B_0 R_0 \tag{13}$$

Combining Equations (10) and (13) gives the poloidal threading current's boundary condition value on the enclosed liquid metal-vacuum interface, in terms of the trapped toroidal flux, Φ, and the boundary's shape:

$$\boxed{I_s = \frac{2\pi}{\mu} \frac{\Phi}{\oint_{\partial S} \frac{z}{r} dr}} \tag{14}$$

The other spatially constant boundary condition value of poloidal threading current is on the exterior surface of the conducting region. It is simply the toroidal field coil system's total ampere-turns, I_{TF}. which is assumed to remain constant in time for this simulation .

The conducting region includes a flowing liquid metal subregion and a solid metal backing subregion. Within each subregion the simulation models the metal conductivity, σ, as a constant value, with different values in different subregions. The boundary condition at the solid/liquid interface requires continuity of the tangential electric field and of the normal current density:

$$\left[\begin{matrix} \frac{n_r}{\sigma_{Liq}} & \frac{n_z}{\sigma_{Liq}} \\ n_z & -n_r \end{matrix}\right]\left(\begin{matrix} \frac{\partial I}{\partial r} \\ \frac{\partial I}{\partial z} \end{matrix}\right)\Bigg|_{Liquid} = \left[\begin{matrix} \frac{n_r}{\sigma_{Sol}} & \frac{n_z}{\sigma_{Sol}} \\ n_z & -n_r \end{matrix}\right]\left(\begin{matrix} \frac{\partial I}{\partial r} \\ \frac{\partial I}{\partial z} \end{matrix}\right)\Bigg|_{Solid} \qquad (15)$$

Here, (n_r, n_z) is a unit vector perpendicular to the solid/liquid interface.

The poloidal current density can be expressed in terms of the "threading current", as

$$\vec{J}_P := J_r\hat{a}_r + J_z\hat{a}_z = \nabla\times\left(\frac{I\hat{\varphi}}{2\pi r}\right) \qquad (16)$$

or in component form,

$$J_r = -\frac{1}{2\pi r}\frac{\partial I}{\partial z} \qquad J_z = +\frac{1}{2\pi r}\frac{\partial I}{\partial r} \qquad (17a,b)$$

which allows the Equation (11) contour integral involving current density to be rewritten as

$$\oint_{\partial S}\frac{\vec{J}}{\sigma}\bullet d\vec{\ell} = \frac{1}{\sigma}\oint_{\partial S}\left(\nabla\times\left(\frac{I\hat{\varphi}}{2\pi r}\right)\right)\bullet d\vec{\ell} = \frac{1}{2\pi\sigma}\oint_{\partial S}\left(\frac{\partial I}{\partial r}\frac{dz}{r} - \frac{\partial I}{\partial z}\frac{dr}{r}\right) \qquad (18)$$

Using Equation (12) for the toroidal field component, the other contour integral in Equation (11) can be rewritten as

$$\oint_{\partial S}\vec{u}\times\vec{B}\bullet d\vec{\ell} =$$

$$= \oint_{\partial S}\left(u_r\hat{a}_r + u_\varphi\hat{\varphi} + u_z\hat{a}_z\right)\times\left(B_r\hat{a}_r + \frac{\mu I}{2\pi r}\hat{\varphi} + B_z\hat{a}_z\right)\bullet\left(\hat{a}_r dr + \hat{a}_z dz\right) = \qquad (19)$$

$$= \oint_{\partial S}\frac{\mu I}{2\pi r}\left(u_r dz - u_z dr\right) + \oint_{\partial S}u_\varphi\left(B_z dr - B_r dz\right)$$

We can also define Ψ, as the net the poloidal magnetic flux between the center line axis of symmetry and any (r,z) location. Then the poloidal field can be written as:

$$\begin{aligned}\vec{B}_P &:= B_r\hat{a}_r + B_z\hat{a}_z \\ &= \nabla\times(\frac{\Psi\hat{\varphi}}{2\pi r})\end{aligned} \tag{20}$$

or in component form, as

$$\begin{aligned}B_r &= -\frac{1}{2\pi r}\frac{\partial\Psi}{\partial z} \\ B_z &= +\frac{1}{2\pi r}\frac{\partial\Psi}{\partial r}\end{aligned} \tag{21a,b}$$

Then the final integral in equation (19) can be rewritten as

$$\begin{aligned}&\oint_{\partial S} u_\varphi(B_z dr - B_r dz) \\ &\qquad = \frac{1}{2\pi}\oint_{\partial S}\frac{u_\varphi}{r}(\frac{\partial\Psi}{\partial r}dr + \frac{\partial\Psi}{\partial z}dz) \\ &\qquad = \frac{1}{2\pi}\oint_{\partial S}\frac{u_\varphi}{r}d\Psi\end{aligned} \tag{22}$$

Combining equations (18), (19) and (22) with (11) results in:

$$\boxed{\frac{d\Phi}{dt} = V_{PS} - \frac{1}{2\pi\sigma}\oint_{\partial S}(\frac{\partial I}{\partial r}\frac{dz}{r} - \frac{\partial I}{\partial z}\frac{dr}{r}) + \frac{\mu I_S}{2\pi}\oint_{\partial S}\frac{(u_r dz - u_z dr}{r}) + \frac{1}{2\pi}\oint_{\partial S}\frac{u_\varphi}{r}d\Psi} \tag{23}$$

Since E_{emf}=0 in the conducting region, the field dynamics there are obtained from Equation (7) and Ampere's law, as:

$$\frac{\partial\vec{B}}{\partial t} = \nabla\times(\vec{u}\times\vec{B}) + \frac{1}{\sigma\mu}\vec{\nabla}^2\vec{B} \tag{24}$$

Fixing attention on the toroidal components,

$$\frac{\partial B_\varphi}{\partial t} = \hat{\varphi}\bullet(\frac{1}{\sigma\mu}\vec{\nabla}^2\vec{B}) + \hat{\varphi}\bullet(\nabla\times(\vec{u}\times\vec{B})) \tag{25}$$

shows the dissipative term is completely independent of the poloidal field,

$$\hat{\varphi}\bullet(\frac{1}{\sigma\mu}\vec{\nabla}^2\vec{B}) = \frac{1}{r}\frac{\partial}{\partial r}(r\frac{\partial}{\partial r}B_\varphi) + \frac{\partial^2 B_\varphi}{\partial z^2} - \frac{B_\varphi}{r^2} \tag{26}$$

and may be rewritten in terms of the poloidal threading current as:

$$\hat{\varphi}\bullet(\frac{1}{\sigma\mu}\bar{\nabla}^2\bar{B}) = \frac{\mu}{2\pi}(\frac{1}{r}\frac{\partial}{\partial r}(r\frac{\partial}{\partial r}(\frac{I}{r})) + \frac{\partial^2}{\partial z^2}(\frac{I}{r}) - \frac{1}{r^2}(\frac{I}{r})) = \frac{\mu}{2\pi r}\Delta^* I \tag{27}$$

where Δ^* is the Grad-Shafranov operator,

$$\Delta^* := r\frac{\partial}{\partial r}\frac{1}{r}\frac{\partial}{\partial r} + \frac{\partial^2}{\partial z^2} \tag{28}$$

Thus the substitution of Equation (27) into Equation (25) gives:

$$\frac{\partial I(r,z,t)}{\partial t} = \frac{1}{\sigma\mu}\Delta^* I(r,z,t) + \frac{2\pi r}{\mu}\hat{\varphi}\bullet(\nabla\times(\bar{u}\times\bar{B})) \tag{29}$$

The last term of Equation (29) can be rewritten in terms of the components, as

$$\frac{2\pi r}{\mu}\hat{\varphi}\bullet(\nabla\times(\bar{u}\times\bar{B})) = -r(\frac{\partial}{\partial r}(\frac{u_r I}{r}) + \frac{\partial}{\partial z}(\frac{u_z I}{r})) + \frac{2\pi r}{\mu}(\frac{\partial}{\partial r}(u_\varphi B_r) + \frac{\partial}{\partial z}(u_\varphi B_z))$$

$$= r(-\frac{u_z}{r}\frac{\partial I}{\partial z} - \frac{u_r}{r}\frac{\partial I}{\partial r} + \frac{u_r I}{r^2} - \frac{I}{r}(\frac{\partial u_r}{\partial r} + \frac{\partial u_z}{\partial z})) + \frac{r}{\mu}(\frac{\partial}{\partial r}(\frac{u_\varphi}{r}(-\frac{\partial\Psi}{\partial z})) + \frac{\partial}{\partial z}(\frac{u_\varphi}{r}\frac{\partial\Psi}{\partial r})) \tag{30}$$

$$= -u_r\frac{\partial I}{\partial r} - u_z\frac{\partial I}{\partial z} + \frac{2u_r I}{r} + \frac{r}{\mu}(\frac{\partial\Psi}{\partial r}\frac{\partial}{\partial z}(\frac{u_\varphi}{r}) - \frac{\partial\Psi}{\partial z}\frac{\partial}{\partial r}(\frac{u_\varphi}{r}))$$

The last terms in Equation (30) can be rewritten as a cross product of gradients:

$$\frac{r}{\mu}(\frac{\partial\Psi}{\partial r}\frac{\partial}{\partial z}(\frac{u_\varphi}{r}) - \frac{\partial\Psi}{\partial z}\frac{\partial}{\partial r}(\frac{u_\varphi}{r})) = \frac{r}{\mu}(\nabla\Psi)\times\nabla(\frac{u_\varphi}{r}) \tag{31}$$

Substituting Equations (30) and (31) into (29) gives the evolution equation for the poloidal threading current variable:

$$\boxed{\frac{\partial I}{\partial t} = -u_r\frac{\partial I}{\partial r} - u_z\frac{\partial I}{\partial z} + \frac{1}{\sigma\mu}\Delta^* I + \frac{2u_r I}{r} + \frac{r}{\mu}\nabla\Psi\times\nabla(\frac{u_\varphi}{r})} \tag{32}$$

Motion of the liquid metal is modeled by the Navier-Stokes equations for incompressible flow with constant properties (e.g. density and viscosity), with body forces including gravity and electromagnetism, and with surface tension effects acting on the free surface. In vector form, where $\bar{u}(r,z,t)$ is the liquid velocity,

$$\nabla\bullet\bar{u} = 0 \tag{33}$$

$$\frac{\partial \bar{u}}{\partial t} + (\bar{u} \bullet \nabla)\bar{u} = -\frac{\nabla p}{\rho} + \nu \bar{\nabla}^2 \bar{u} + \bar{g} + \frac{\bar{J} \times \bar{B}}{\rho} \tag{34}$$

where $\bar{g} = g_z \hat{a}_z$ with g_z=-9.8 m/s^2 on the earth's surface. There is a "no-slip" boundary condition specifying the liquid velocity on all stationary material surfaces,

$$(\bar{u}(\bullet, t)|_{MaterialSurface} = 0 \tag{35}$$

The pressure "boundary condition" on the free surface is

$$p|_{FreeSurface} = \gamma(\frac{1}{R_1} + \frac{1}{R2}) \tag{36}$$

where R_1 and R_2 are the surface's local radii of curvature and the surface tension parameter, γ, is a material constant.

The electromagnetic force can be resolved into cylindrical components as follows:

$$\begin{aligned} \bar{J} \times \bar{B} &= [-\frac{1}{2\pi r}\frac{\partial I}{\partial z}\hat{a}_r + J_\varphi \hat{\varphi} + \frac{1}{2\pi r}\frac{\partial I}{\partial r}\hat{a}_z] \quad \times \quad [B_r \hat{a}_r + \frac{\mu I}{2\pi r}\hat{\varphi} + B_z \hat{a}_z] \\ &= \{J_\varphi B_z - (\frac{1}{2\pi r}\frac{\partial I}{\partial r})(\frac{\mu I}{2\pi r})\}\hat{a}_r \\ &\quad + \{(\frac{1}{2\pi r}\frac{\partial I}{\partial r})B_r - (-\frac{1}{2\pi r}\frac{\partial I}{\partial z})B_z\}\hat{\varphi} \\ &\quad + \{(-\frac{1}{2\pi r}\frac{\partial I}{\partial z})(\frac{\mu I}{2\pi r}) - B_r J_\varphi\}\hat{a}_z \end{aligned} \tag{37}$$

Axisymmetric equations (34) and (35) can be written in cylindrical coordinates component form as follows:

$$\frac{1}{r}\frac{\partial (r u_r)}{\partial r} + \frac{\partial u_z}{\partial z} = 0 \tag{38}$$

$$\begin{aligned} \frac{\partial u_r}{\partial t} &= \frac{u_\varphi^2}{r} - u_r \frac{\partial u_r}{\partial r} - u_z \frac{\partial u_r}{\partial z} - \frac{1}{\rho}\frac{\partial p}{\partial r} + \nu(\frac{1}{r}\frac{\partial}{\partial r}(r\frac{\partial u_r}{\partial r}) + \frac{\partial^2 u_r}{\partial z^2} - \frac{u_r}{r^2}) \\ &\quad + \frac{J_\varphi B_z}{\rho} - \frac{\mu I}{4\pi^2 r^2 \rho}\frac{\partial I}{\partial r} \end{aligned} \tag{39}$$

$$\begin{aligned} \frac{\partial u_\varphi}{\partial t} &= -\frac{u_r u_\varphi}{r} - u_r \frac{\partial u_\varphi}{\partial r} - u_z \frac{\partial u_\varphi}{\partial z} + \nu(\frac{1}{r}\frac{\partial}{\partial r}(r\frac{\partial u_\varphi}{\partial r}) + \frac{\partial^2 u_\varphi}{\partial z^2} - \frac{u_\varphi}{r^2}) \\ &\quad + \frac{1}{2\pi r \rho}(\frac{\partial I}{\partial r}B_r + \frac{\partial I}{\partial z}B_z\} \end{aligned} \tag{40}$$